



OPEN ACCESS

EDITED BY

Qinsheng Wei,
Ministry of Natural Resources, China

REVIEWED BY

Rui Bao,
Ocean University of China, China
Yin Xijie,
State Oceanic Administration, China
Youcheng Bai,
Ministry of Natural Resources, China

*CORRESPONDENCE

Fajin Chen
✉ fjchen@gdou.edu.cn

RECEIVED 31 July 2024

ACCEPTED 09 October 2024

PUBLISHED 11 November 2024

CITATION

Cao R, Lao Q, Huang C, Han J, Jin G, Lu X, Cai M, Chen C and Chen F (2024) Source apportionment of organic carbon and black carbon in the surface sediments of the Pearl River Estuary and its adjacent South China Sea: insight from stable carbon and nitrogen isotopes.
Front. Mar. Sci. 11:1473466.
doi: 10.3389/fmars.2024.1473466

COPYRIGHT

© 2024 Cao, Lao, Huang, Han, Jin, Lu, Cai, Chen and Chen. This is an open-access article distributed under the terms of the [Creative Commons Attribution License \(CC BY\)](https://creativecommons.org/licenses/by/4.0/). The use, distribution or reproduction in other forums is permitted, provided the original author(s) and the copyright owner(s) are credited and that the original publication in this journal is cited, in accordance with accepted academic practice. No use, distribution or reproduction is permitted which does not comply with these terms.

Source apportionment of organic carbon and black carbon in the surface sediments of the Pearl River Estuary and its adjacent South China Sea: insight from stable carbon and nitrogen isotopes

Ruixue Cao^{1,2,3}, Qibin Lao^{1,2,3}, Chao Huang^{1,2,3}, Jiajun Han¹, Guangzhe Jin^{1,2,3}, Xuan Lu⁴, Minggang Cai^{1,5}, Chunqing Chen¹ and Fajin Chen^{1,2,3*}

¹College of Ocean and Meteorology, Guangdong Ocean University, Zhanjiang, China, ²Key Laboratory for Coastal Ocean Variation and Disaster Prediction, Guangdong Ocean University, Zhanjiang, China, ³Key Laboratory of Climate, Resources and Environment in Continental Shelf Sea and Deep Sea of Department of Education of Guangdong Province, Guangdong Ocean University, Zhanjiang, China, ⁴Polar and Marine Research Institute, College of Harbor and Coastal Engineering, Jimei University, Xiamen, China, ⁵State Key Laboratory of Marine Environmental Science, College of Ocean and Earth Sciences, Xiamen University, Xiamen, China

Coastal estuaries and adjacent continental shelf seas constitute vital global carbon reservoirs, and the sources and transformations of organic carbon in these regions are crucial to global biogeochemical cycles and climate change. This study investigated the total organic carbon (TOC), total nitrogen (TN), black carbon (BC), and their stable carbon and nitrogen isotopes ($\delta^{15}\text{N}_{\text{TN}}$, $\delta^{13}\text{C}_{\text{TOC}}$, $\delta^{13}\text{C}_{\text{BC}}$) in the surface sediments of the Pearl River Estuary (PRE) and its adjacent northern South China Sea (NSCS) aiming to assess the impact of human activities on organic carbon dynamics in these areas. Results showed that the highest TOC concentrations occurred in the inner PRE due to intense human activities, and decreased seaward. The west side of the PRE exhibited higher TOC levels than the east side, which was attributed to differences in hydrodynamic processes and human activities. The westward flow of the Pearl River diluted water, which carried terrestrial organic matter inputs due to the influence of the Coriolis effect and intense local human activities, was a primary contributor to higher TOC levels on the west side (terrestrial source). In contrast, increased productivity and intensive mariculture activities on the east side predominated as sources of organic matter (marine source). Similar to the TOC, BC and TN sources were mainly influenced by human activities. $\delta^{15}\text{N}_{\text{TN}}$ distribution shows that TN in the east side of PRE mainly originated from industrial wastewater input from the Pearl River, while in the east side TN was mainly from domestic sewage discharge. Additionally, BC sources have shifted from primarily biomass combustion in the 1990s to fossil fuel emissions presently. Isotopic analysis revealed that over 70%

of BC originated from fossil fuel inputs and C3 plant combustion, highlighting the significant influence of human activities in the PRE and adjacent NSCS, and underscoring the need for effective management and protection of the environment in these regions.

KEYWORDS

organic matter, total organic carbon, black carbon, stable isotopes, Pearl River Estuary

Introduction

Estuaries and coastal areas, situated between the land and the ocean, are key areas for transporting terrestrial materials to the ocean. Total organic matter (TOC) in marine sediments is crucial factor for global biogenic cycling and climate change (Atwood et al., 2020; LaRowe et al., 2020; Faust et al., 2021). According to reports, approximately 90% of organic carbon is buried in estuaries and coastal shelf areas, making it one of the most important carbon reservoirs in the global ocean and playing a crucial role in global carbon cycling and climate change (Dai et al., 2022; LaRowe et al., 2020; Zhao et al., 2021). Among the organic matter, black carbon (BC) is a critical component of sedimentary organic matter, which mainly originates from the incomplete combustion of fossil fuels and biomass, and/or from weathered rocks (Coppola et al., 2022; Dickens et al., 2004; Pang et al., 2021). Moreover, due to its remarkable stability in the carbon pool, BC serves as a potent tracer of human activities across both modern and geological timeframes (Wu et al., 2019; Dan et al., 2022; Sun et al., 2022). Therefore, studying the sources and fate of organic carbon in coastal marine sediments can contribute to a deeper understanding of global ocean carbon burial and its impact on climate change.

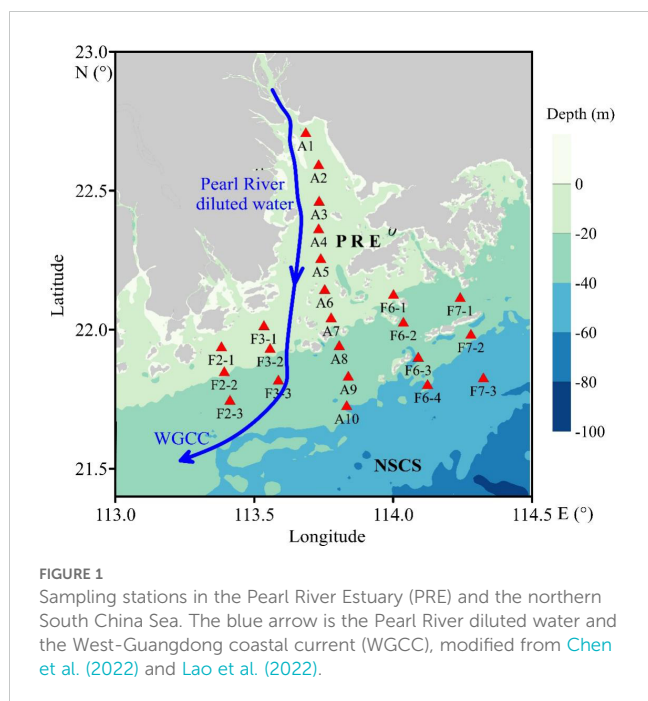
However, the complexity of hydrodynamics in coastal areas, especially in estuarine areas, and the impact of intense human activities, have posed challenges in identifying the sources of organic carbon in coastal areas. The development in use of stable isotopes (e.g., carbon and nitrogen isotopes) has facilitated a deeper understanding of coastal marine organic matter sources, because their compositions can effectively differentiate the origins of marine sedimentary organic carbon (Carneiro et al., 2021; Liu et al., 2019; Pang et al., 2021; Xia et al., 2021; Yang et al., 2023). For example, the carbon isotope abundance of TOC ($\delta^{13}\text{C}_{\text{TOC}}$) in marine organic matter (from -21‰ to -19‰) is significantly higher than that of terrestrial organic matter (from -30‰ to -23‰) (Meyers, 1994). Similarly, the black carbon isotopes ($\delta^{13}\text{C}_{\text{BC}}$) produced by incomplete combustion of C3 plants (-26.7‰) are significantly lower than those produced by fossil fuel combustion (-25.2‰) and rock weathering (-20.2‰) (Dickens et al., 2004; Vaezzadeh et al., 2023; Xiao et al., 2021; Uchida et al., 2023). Thus, the stable carbon isotope in the organic matter can be a valuable tool for tracing the complex organic sources in coastal marine ecosystems.

The Pearl River Estuary (PRE) is an interface connecting the developed economic zone of South China with the northern South China Sea (NSCS). This is a highly dynamic estuarine system, carrying the input of the Pearl River, the second-largest runoff in China. In particular, under the influence of the Coriolis force, the Pearl River diluted water tends to flow to the west, which leads to obvious differences in pollutant loads and biogeochemical processes between the east and west sides of the PRE (Ye et al., 2015 and 2017). Despite intense human activities, current research has provided some insights into the distribution and burial patterns of organic matter in the PRE, as influenced by salinity gradients (Xiao et al., 2022; Yin et al., 2021; Wei et al., 2020; Li et al., 2023). However, under the complex hydrodynamic conditions of the PRE, it is still unclear whether the obvious hydrodynamic differences between the east and west sides of the PRE will lead to the difference in the source and fate of marine organic matter between the two sides. Particularly, with the rapid development of the Pearl River Delta (such as the development of the Guangdong-Hong Kong-Macao Greater Bay Area), changes in human activities may also change the source and fate of these organic matter (Li et al., 2023; Yang et al., 2023). Thus, conducting additional field investigations is imperative to unravel the sources and burial processes of organic carbon in the PRE and its neighboring regions. In this study, TOC, total nitrogen (TN), BC, and their stable carbon and nitrogen isotopes ($\delta^{15}\text{N}_{\text{TN}}$, $\delta^{13}\text{C}_{\text{TOC}}$ and $\delta^{13}\text{C}_{\text{BC}}$) in the surface sediments of the PRE and its adjacent NSCS were investigated to explore the impact of increasingly intense human activities on the sources and burial of organic carbon in these regions.

Materials and methods

Field sampling

The study area encompassed the upper reaches of the PRE to the offshore areas of the NSCS, as illustrated in Figure 1. During August 2021, a total of 23 surface sediment samples, collected from the upper 0.5 cm layer at 23 stations spanning the PRE and its adjacent offshore areas within the NSCS (21.74°N to 22.71°N, 113.38°E to 114.32°E), were obtained using a box sampler. After collection, the samples were stored at -20°C onboard the ship for subsequent laboratory analysis.



After on-site sampling was concluded, the sediment samples were promptly transferred to the laboratory and immediately freeze-dried for subsequent analysis.

Sediment grain size

An appropriate amount of freeze-dried sediment sample was weighed and placed in a centrifuge tube. Then, 10 ml of 10% H_2O_2 solution was added, and the sediment samples were placed in a 60°C water bath for 24 hours to remove organic matter. Subsequently, 10% HCl was added to dissolve carbonates. The sediment samples were then rinsed with deionized water and dispersed with 0.05 mol L^{-1} $(NaPO_3)_6$ using an ultrasonic bath. The grain size distribution was analyzed using a particle size analyzer (Master Sizer 3000) ([Yang et al., 2023](#)).

Measurements for TOC, TN and their isotopes

For TOC and its carbon isotope ($\delta^{13}C_{TOC}$), the sediment samples underwent pretreatment with diluted HCl to remove carbonates. TN and its nitrogen isotope ($\delta^{15}N_{TN}$) were measured in bulk samples. TOC, TN, $\delta^{13}C_{TOC}$, and $\delta^{15}N_{TN}$ were determined using an elemental analysis isotope ratio mass spectrometer (EA Isolink series elemental analyzer interfaced with a MAT 253 plus mass spectrometer). The values of $\delta^{15}N_{TN}$ and $\delta^{13}C_{TOC}$ were reported relative to atmospheric N_2 and the Vienna PeeDee Belemnite standard (V-PDB), respectively. Reference standards IVA33802151 and AEB2153 were used to ensure the accuracy and precision of TOC and TN, respectively. The average standard

deviations of TOC and TN were $\pm 0.2\%$, and those of $\delta^{15}N_{TN}$ and $\delta^{13}C_{TOC}$ were $\pm 0.2\%$.

Measurements for black carbon and its isotopes

The pretreatment of BC and its carbon isotope ($\delta^{13}C_{BC}$) followed the chemical oxidation method by [Lim and Cachier \(1996\)](#). First, sediment samples were ground to 200 mesh and 10 mL of 3 mol L^{-1} HCl were added to remove carbonates. Then, a mixed solution of 10 mL of hydrofluoric acid (HF, 48%) and HCl (6 mol L^{-1}) was injected to react thoroughly for 48 hours, with shaking every 2 hours. Subsequently, 10 mL of 10 mol L^{-1} HCl was added for 24 hours to remove secondary fluoride. Finally, a mixed solution of sulfuric acid (H_2SO_4 , 2 mol L^{-1}) and potassium dichromate ($K_2Cr_2O_7$, 0.1 mol L^{-1}) was added and the samples were placed in an ultrasonic water bath at 55°C for 60 hours to remove kerogen and organic matter. The BC and $\delta^{13}C_{BC}$ were measured using the EA-Isolink series elemental analyzer interfaced with a MAT 253 plus mass spectrometer. The values of $\delta^{13}C_{BC}$ were reported relative to the V-PDB standard. Precision was monitored using the reference standard IVA33802151. The average standard deviations of BC and $\delta^{13}C_{BC}$ were $\pm 0.2\%$ and $\pm 0.1\%$, respectively.

Data statistical analysis

Correlation analysis and scatter plot drawing were performed using IBM SPSS (version 19). The spatial distribution characteristics of carbon, nitrogen, and their isotopes were plotted using Ocean Data View (version 4). The contribution of the potential sources of black carbon in sediments was estimated using the IsoSource model.

Results

The distribution of sediment grain size

The average particle size (M_z) of sediment in the PRE and adjacent NSCS waters, ranging from 12.0 to 49.2 μm , was calculated using the method proposed by [Folk and Ward \(1957\)](#) ([Figure 2](#)). The sediments at all sites primarily composed of silt, ranging in percentages from 58.39% to 94.55% ([Figures 2A–D](#)). In contrast, sand and clay contents in the PRE and adjacent offshore NSCS were relatively lower, with sand contents varying from 1.33% to 31.77% and clay contents ranging from 2.94% to 25.39%, respectively ([Figures 2B, D](#)). The distributions of M_z and sand content were similar, showing lower in the inner PRE and gradually increasing seawards ([Figures 2A, D](#)). Conversely, the contents of clay and silt were higher in the inner PRE and lower in the offshore NSCS regions ([Figures 2B, C](#)). Notably, sites A6 and A10 exhibited the lowest clay content, whereas site A6 had the highest silt content. At stations A7, A8, and A10, the silt contents were significantly lower, showing a distinct inverse relationship with the distribution of sand.

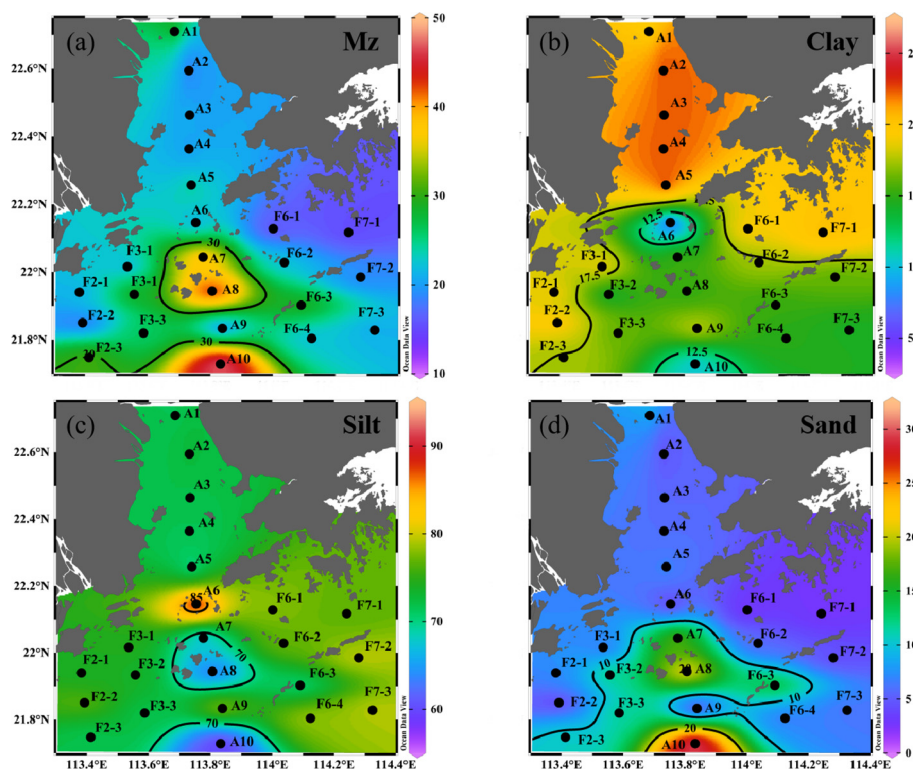


FIGURE 2
The spatial distribution characteristics of Mz (A), clay (B), silt (C) and sand (D) in the PRE and its adjacent offshore NSCS.

The distribution of total nitrogen and organic carbon and their isotopes

The distributions of TOC, TN, and BC contents, along with their isotopes $\delta^{15}\text{N}_{\text{TN}}$, $\delta^{13}\text{C}_{\text{TOC}}$, and $\delta^{13}\text{C}_{\text{BC}}$, as well as C/N (TOC/TN) and BC/TOC ratios in the surface sediments of the PRE and the adjacent offshore NSCS displayed varying patterns (Figure 3). TOC and TN contents ranged from 0.3% to 1.3% and 0.03% to 0.13%, with averages of 0.87% and 0.096%, respectively. The highest TOC content was found in the inner PRE, with higher concentrations also observed in the western and eastern parts, whereas lower content was observed in the offshore areas (Figure 3A). Conversely, higher TN contents were noted in the western and eastern parts of the PRE, while lower concentrations were found toward the offshore NSCS regions (Figure 3B). The $\delta^{13}\text{C}_{\text{TOC}}$ and $\delta^{15}\text{N}_{\text{TN}}$ values varied from -26.0‰ to -21.9‰ and from 4.8‰ to 5.9‰, respectively, with average values of -23.1‰ and 5.3‰ in the PRE and adjacent offshore NSCS regions. The lowest $\delta^{13}\text{C}_{\text{TOC}}$ values occurred in the upper PRE, increasing seawards (Figure 3C). Similarly, lower $\delta^{15}\text{N}_{\text{TN}}$ values were observed in the PRE, with values increasing seaward (Figure 3D). Notably, the western PRE exhibited lower $\delta^{13}\text{C}_{\text{TOC}}$ and $\delta^{15}\text{N}_{\text{TN}}$ values, while higher values were observed in the eastern PRE (Figures 3C, D).

BC contents ranged from 0.19% to 0.42% in the PRE and adjacent offshore NSCS regions, with an average of 0.30%. In contrast to TOC and TN, lower BC contents were noted in the

inner PRE, gradually increasing towards the outer offshore regions (Figure 3E). The $\delta^{13}\text{C}_{\text{BC}}$ values ranged from -25.7‰ to -23.0‰, with an average of -23.5‰. Similar to the distribution of BC contents, lower $\delta^{13}\text{C}_{\text{BC}}$ values were found in the inner PRE, and values gradually increased seawards (Figure 3F).

C/N ratios ranged from 8.29 to 15.62, with an average of 10.88. Contrary to the $\delta^{13}\text{C}_{\text{TOC}}$ distribution, higher C/N ratios were observed in the inner PRE, decreasing seaward (Figure 3G). The BC/TOC ratios ranged from 0.24 to 1.04, with an average of 0.35. Lower BC/TOC ratios were observed in the inner PRE, whereas higher ratios were observed in the outer offshore regions (Figure 3H).

Discussion

Source apportionment of organic matter sources

The TOC content in the PRE is close to that in the coastal areas of western Guangdong Province (0.9%) (Gu et al., 2010), but higher than the coastal areas of eastern Guangdong Province, such as Daya Bay (0.6%) (Yang et al., 2023). The distribution pattern of TOC in our study is agreeable with this distribution characteristics of low in the east and high in the west (Figure 3). Additionally, the TOC content in our study is higher than that in the Leizhou Peninsula (0.42%) (Xia et al., 2022), the Bohai Sea (0.46%) (Gao et al., 2016),

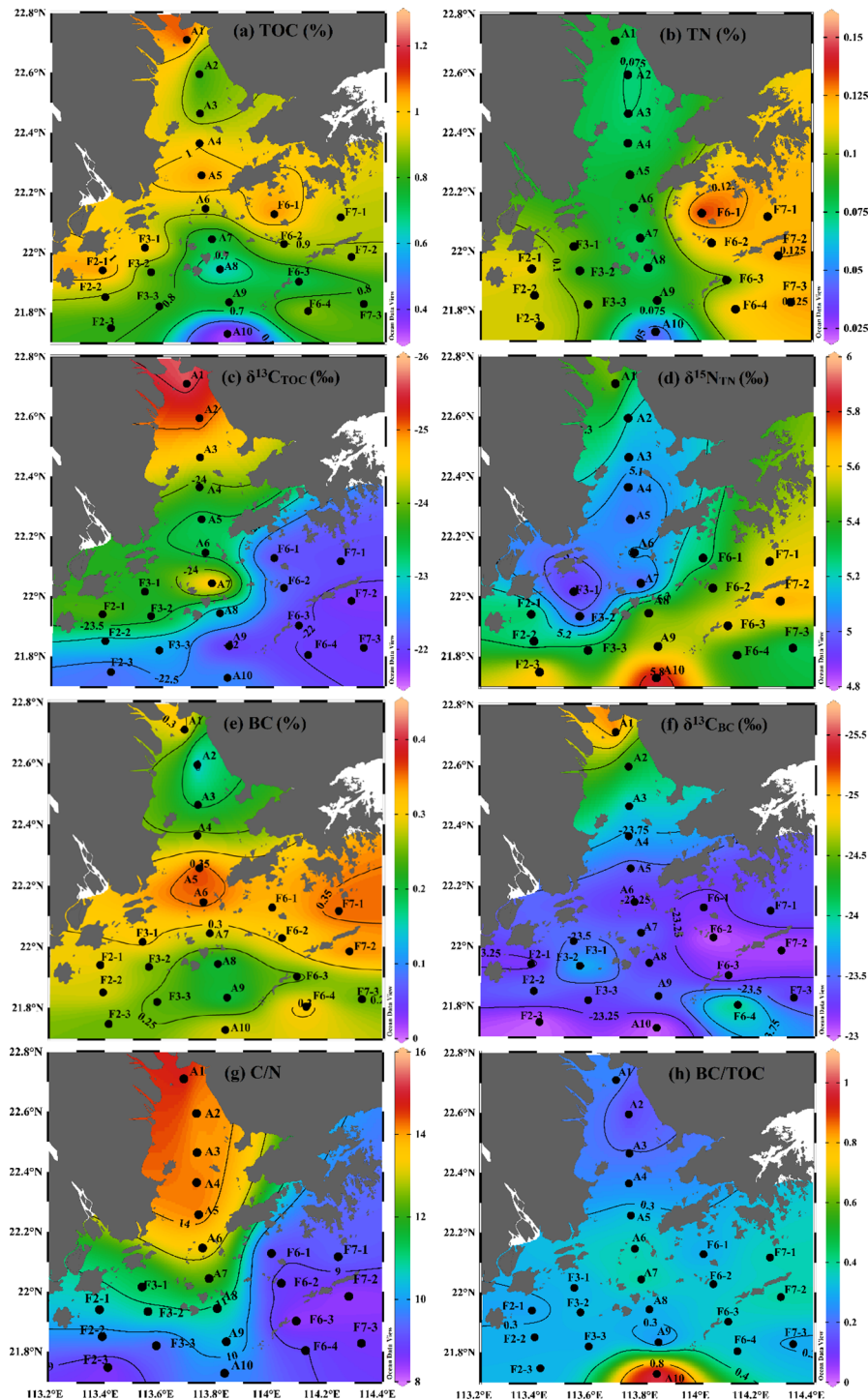


FIGURE 3

The spatial distribution characteristics of TOC (A), TN (B), clack carbon (E) and their isotopic values (C, D, F), and C/N (G) and BC/TOC (H) ratios in the PRE and its adjacent offshore NSCs.

the Yellow Sea (0.50%) (Zhang et al., 2014), and the Western Taiwan Strait (0.37%) (Ye et al., 2011). Similarly, the TN content in the PRE is higher than that Leizhou Peninsula (0.05%) (Xia et al., 2022) and the Bohai Sea (0.07%) (Gao et al., 2016). This reflects that the organic matter within the sediment of the PRE may be significantly more impacted by human activities.

This study delves into the intricate influence of human activities on the distribution patterns of organic matter within the PRE and its adjacent waters. It revealed a significant positive correlation between TOC and TN contents (Figure 4A), suggesting similar sources for these components (Xia et al., 2022; Yang et al., 2023). However, the TOC-TN slope of 5.02 significantly deviates from the

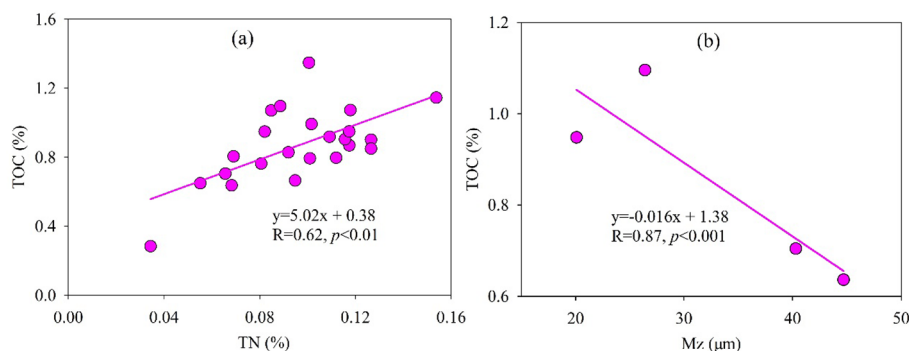


FIGURE 4

The linear correlation of TOC-TN (A) and TOC-Mz (B) in the PRE and its adjacent offshore NSCS.

Redfield value (6.8), indicating the complexity and diversity of organic matter sources in the PRE, which are influenced by human activities (Zhang et al., 2009; Li et al., 2023). Geochemical indices such as C/N ratios and stable carbon and nitrogen isotopes ($\delta^{15}\text{N}_{\text{TN}}$ and $\delta^{13}\text{C}_{\text{TOC}}$) are crucial tools for distinguishing between terrestrial and marine sources of organic matter in aquatic environments (Carneiro et al., 2021; Lao et al., 2023a; Wu et al., 2023; Xia et al., 2021). Typically, C/N ratios for marine sources like phytoplankton and zooplankton range from 3–8, whereas terrestrial sources generally display higher values (≥ 12) (Meyers, 1994). Additionally, terrestrial and marine sources exhibit distinct isotopic signatures. Terrestrial plants, categorized into C3 and C4 types, show $\delta^{13}\text{C}_{\text{TOC}}$ values ranging from -30‰ to -23‰ for C3 plants and from -16‰ to -10‰ for C4 plants (O'Leary, 1988). In contrast, $\delta^{13}\text{C}_{\text{TOC}}$ values from marine organic matter sources range from -22‰ to -19‰ (Fontugne and Jouanneau, 1987).

In the PRE and its adjacent waters, C/N ratios and $\delta^{13}\text{C}_{\text{TOC}}$ values closely align with terrestrial sources. Particularly in the PRE (stations A1–A8), the C/N ratios consistently exceeded 12, indicating a predominant input of terrestrial organic matter. Notably, the significantly higher C/N ratios (>12) in the western PRE compared to those (<9) in the eastern PRE suggested a stronger terrestrial influence in the west, contrasting with the dominant marine sources in the east. Additionally, higher $\delta^{13}\text{C}_{\text{TOC}}$ values in the eastern PRE (from -22.7‰ to -21.9‰) indicated a dominance of marine sources, whereas the lower values in the western PRE (from -24.0‰ to -22.3‰) suggested proximity to terrestrial C3 plants.

Similarly, $\delta^{15}\text{N}_{\text{TN}}$ values were lower in the inner PRE, and the values decreased seaward (Figure 3). Additionally, the $\delta^{15}\text{N}_{\text{TN}}$ values in the west side of PRE were lower than that in the east side (Figure 3). Generally, the industrial waste is characterized by low $\delta^{15}\text{N}_{\text{TN}}$ value (Yang et al., 2023) and previous studies attributed the low $\delta^{15}\text{N}_{\text{TN}}$ values in the coastal sediments to the river discharge (Yang et al., 2023). In contrast, domestic sewage exhibits relatively high $\delta^{15}\text{N}_{\text{TN}}$ values (Lao et al., 2023a). As the second largest runoff river in China, the Pearl River can discharge a large amount of wastewater from the basin into the PRE. This led to the trend of decreasing ammonium concentration from PRE to offshore (Chen et al., 2022). Thus, the lower $\delta^{15}\text{N}_{\text{TN}}$ values in the west side of PRE

could reflect the influence of industrial waste input. However, the eastern areas of the PRE gather one of the most developed urban agglomerations in China, and the domestic sewage of these cities may be responsible for the high $\delta^{15}\text{N}_{\text{TN}}$ value in the east side of the PRE (Ye et al., 2015 and 2017).

Impact of human activities and hydrodynamic processes on organic matter

In the summer, the flood season for the Pearl River basin, a substantial influx of land-based pollutants flows into the PRE and its adjacent waters (Chen et al., 2022; Li et al., 2019; Ye et al., 2017 and 2018; Zhang et al., 2009). Hydrodynamic processes and human activities are two primary factors contributing to the regional disparity in organic matter distribution within the PRE. The Pearl River runoff, influenced by the Coriolis force of the Northern Hemisphere, shifts westward upon entering the PRE, contributing to the formation of the West-Guangdong coastal current (Deng et al., 2022; Lao et al., 2023b; Ye et al., 2015 and 2016). As a result, the western PRE accumulates a significant amount of pollutants, including organic matter (Ye et al., 2017 and 2018). Furthermore, the rapid economic growth on the western side of the PRE and in the coastal area of western Guangdong has increased pollutant inputs from terrestrial sources in recent years, surpassing those from the coastal current and becoming the predominant source of pollutants in these regions (Lao et al., 2019; Zhou et al., 2024). Thus, these factors collectively influence the organic matter content on the western side of the PRE, resulting in higher concentrations compared to the eastern side.

The Pearl River Delta and the Pearl River Basin have undergone significant economic development, increasing the human influence on the organic matter in the PRE and its adjacent areas (Ye et al., 2017 and 2018). Since the 1980s, large-scale development activities such as land reclamation, river sand mining, and construction of ports, docks, and sea-crossing bridges have led to a substantial influx of terrestrial organic matter into these waters (Ye et al., 2017 and 2018). Despite these large-scale development activities, TOC contents decrease as they move seaward (Figure 3), reflecting a

diminishing human impact in the offshore. Notably, TOC contents at stations A2 and A3, near the Chiwan Container Terminal in Shenzhen, are lower, likely due to frequent disturbances from ship navigation and dredging activities. These disturbances can cause resuspension of deposited organic matter, resulting in the ongoing remineralization and degradation of the matter (Lao et al., 2023a), which in turn results in coarser sediment particles. A significant negative correlation between TOC content and Mz further supports this observation about the influence of human activities (Figure 4B).

However, the increase in $\delta^{13}\text{C}_{\text{TOC}}$ values toward the offshore areas (Figure 3) indicates that a shift in the dominant source of organic matter towards marine source in these regions. Although the TOC content on the eastern side of the PRE is relatively lower compared to the western side, it remains significantly higher than in the offshore areas, with notably higher $\delta^{13}\text{C}_{\text{TOC}}$ values than those in the western region (Figure 3). This difference in TOC content and $\delta^{13}\text{C}_{\text{TOC}}$ values can be attributed to two main factors. Firstly, the eastern region experiences less hydrodynamic disturbance. This is due to the minimal influence of the Pearl River diluted water input, which facilitates phytoplankton growth (Ye et al., 2015 and 2016). This condition is corroborated by the observed higher marine productivity on the east side of the PRE (Ye et al., 2015). Increased oceanic productivity promotes biological activity, and the deposition and burial of the resulting organic debris significantly contribute to the elevated TOC levels in this region. Additionally, the eastern region serves as a crucial aquaculture base, benefiting from its high productivity. The excrement and biological debris from aquaculture organisms are significant contributors to the high TOC content (0.4–1.2%) in this area (Yang et al., 2023; Huang et al., 2020 and 2021). Previous studies have indicated that organic matter from aquaculture areas tends to be finer than that naturally deposited in non-aquaculture zones (Biggs and Howell, 1984). Furthermore, the weaker hydrodynamic conditions compared to the western region facilitate the burial of organic matter in sediments through biological deposition (Yang et al., 2023). Therefore, despite the relatively minor terrestrial organic matter input in the eastern region, the high rates of biological deposition and burial result in relatively high organic matter content.

Consequently, while the organic matter contents on both the west and east sides of the PRE are elevated, their sources differ significantly. Influenced by hydrodynamic processes, the elevated organic matter content on the west side primarily stems from terrestrial inputs and local human activities. Conversely, the increased marine productivity and human aquaculture activities in the area largely contribute to the higher organic matter content on the east side. Nonetheless, these variations are all ultimately linked to the impact of human activities.

The sources of black carbon in the PRE dominated by human activities

The spatial distribution pattern of BC is slightly different from TOC (Figure 3). Although the higher value of BC also occurred in the inner PRE and the western side of the PRE, the higher content of BC also occurred in the eastern side (Figure 3E). Similar to the

TOC, the higher BC in the inner PRE and the western side of the PRE could be related to the intense human activities. Biomass fuels and fossil fuels are considered as the two main BC sources in the marine environment (Yang et al., 2023). The coastal areas in the eastern side of the PRE is one of the most developed areas in China, which is greatly affected by human activities in industry and ports. Previous studies have confirmed that regions with coal-fired power plants and high shipping activities have high BC content in the sedimentary environment (Yang et al., 2023; Marlon et al., 2008). This may be the reason for the higher BC content on the east side of PRE. Similar anomalous high values of BC also observed in the Daya Bay on the east side of PRE (Yang et al., 2023).

The origins of BC in the PRE can typically be traced using the BC/TOC ratio and $\delta^{13}\text{C}_{\text{BC}}$ values (Liu et al., 2019; Wu et al., 2019). Generally, the BC/TOC ratio from biomass fuels (~0.1) is lower than that from fossil fuels (~0.5) (Ruellan and Cachier, 2001; Bucheli et al., 2004). Additionally, isotope analysis can further differentiate BC sources, as each type exhibits distinct isotopic signatures. The $\delta^{13}\text{C}_{\text{BC}}$ values for BC derived from the combustion of C3 and C4 plants range from -30.7‰ to -23.7‰ and from -14.3‰ to -10.1‰, respectively, with average values of -27.2‰ and -12.2‰ (Dickens et al., 2004; Vaezzadeh et al., 2023). The average $\delta^{13}\text{C}_{\text{BC}}$ value resulting from the combustion of fossil fuels is -25.2‰ (Dickens et al., 2004). This study observed a significant positive correlation between $\delta^{13}\text{C}_{\text{TOC}}$ and $\delta^{13}\text{C}_{\text{BC}}$ in the PRE and adjacent areas (Figure 5A), suggesting that BC in the sediments primarily originates from the combustion of fossil fuels,

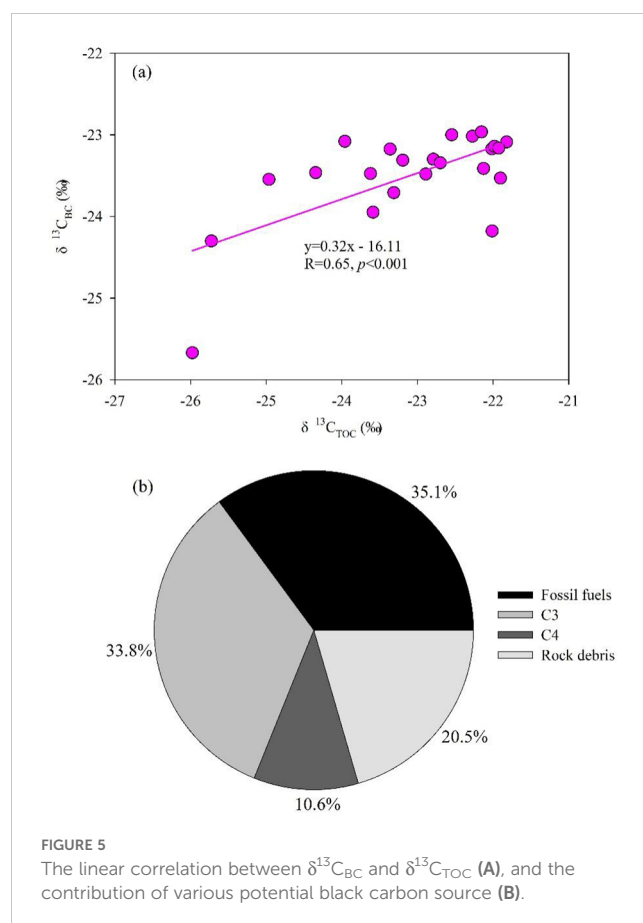


FIGURE 5 The linear correlation between $\delta^{13}\text{C}_{\text{BC}}$ and $\delta^{13}\text{C}_{\text{TOC}}$ (A), and the contribution of various potential black carbon source (B).

with a significant contribution from biomass as well (Yang et al., 2023). Moreover, the BC/TOC ratios, ranging from 0.24 to 1.04 with an average of 0.35, align more closely with fossil fuel sources. Notably, compared to the BC/TOC ratio of 0.23 recorded in 1990, the current ratios in the PRE have significantly increased, suggesting a recent shift in energy structure towards greater reliance on fossil fuels. Furthermore, $\delta^{13}\text{C}_{\text{BC}}$ values ranging from -25.7‰ to -23.0‰ fall within the isotopic range of C3 plants and fossil fuels, supporting the dominance of fossil fuel emissions driven by human activities as the main source of black carbon in the PRE. With the rapid development of the socio economy, fossil fuel emissions continue to increase globally, especially in East Asia (Song et al., 2021). These polluted aerosols would eventually settle into the surface and marine environment (Lao et al., 2024), including the PRE region (Sun et al., 2008).

As depicted in Figure 3, the $\delta^{13}\text{C}_{\text{BC}}$ values display a gradual increasing trend as they move from the estuary towards the open sea, indicating a potential change in BC sources. The considerable isotopic difference between C3 plants and fossil fuels allows the spatial distribution of $\delta^{13}\text{C}_{\text{BC}}$ values to reflect changes in BC types in the sediments. In the estuarine area, terrestrial inputs have a greater impact, accumulating substantial terrestrial organic matter, including carbon debris from C3 plant combustion (coarse particle components produced by biomass fuel combustion) (Yang et al., 2023). Conversely, BC in the offshore area likely receives more deposition from soot (fine particle components produced by fossil fuel combustion) (Fu et al., 2023; Liu et al., 2024; Zhang et al., 2024).

To further ascertain the sources of BC in the PRE sediments, this study employed the IsoSource model to estimate the contributions from various sources. Previous studies suggested that C3 plants are the primary source of terrestrial organic matter in the PRE and adjacent waters (Yu et al., 2010; Dan et al., 2022). However, with the massive use of fossil fuels, their contribution cannot be ignored, and even become the main source of organic matter in some areas of the PRE (Yang et al., 2023). Therefore, the model uses end-member $\delta^{13}\text{C}_{\text{BC}}$ values for fossil fuels, C3 plants, C4 plants, and rock debris as -25.2‰, -26.7‰, -14.0‰, and -20.2‰, respectively, derived from the literatures (Dickens et al., 2004; Vaezzadeh et al., 2023; Xiao et al., 2021; Uchida et al., 2023). The calculation formula is as follows:

$$\delta_M = f_A \delta_A + f_B \delta_B + f_C \delta_C + f_D \delta_D \quad (1)$$

$$1 = f_A + f_B + f_C + f_D \quad (2)$$

Here, δ_M represents the measured $\delta^{13}\text{C}_{\text{BC}}$ values, δ_A , δ_B , δ_C , and δ_D are the $\delta^{13}\text{C}_{\text{BC}}$ values from the end-members of fossil fuels, C3 plants, C4 plants, and rock debris, respectively, and f represents the proportional contribution of each potential source. Results revealed that fossil fuels (35.1%) and C3 plants (33.8%) were the primary sources of black carbon in the PRE, with rock debris contributing 20.5%, and C4 plants accounting for only 10.6% of the total (Figure 5B). The high contribution of anthropogenic emissions is similar to the current quantitative results in the adjacent waters of

the PRE (Yang et al., 2023). Nearly 70% of the black carbon present in the surface sediments can be attributed to the combustion of fossil fuels and C3 plants, unequivocally highlighting the profound influence of human activities on the sources of BC in the PRE.

Conclusion

This study analyzed TOC, TN, BC, and their stable carbon and nitrogen isotopes in the surface sediments of the PRE and its adjacent NSCS. The purpose was to evaluate the impact of human activities on organic matter in these regions. Generally, TOC content is higher in the inner regions of the PRE and gradually decreases towards the offshore areas. The TOC content is notably higher on the west side of the PRE than that on the east side, largely due to varying hydrodynamic processes and the intense human activities on the west side. Influenced by the Coriolis force, the high TOC levels on the west side are primarily attributed to terrestrial organic matter inputs from the westward flow of Pearl River diluted water, as well as intense local human activities. In contrast, on the east side of the PRE, elevated TOC levels are contributed by higher productivity and intensive mariculture activities. Additionally, the distribution of BC and TN is closely correlated with TOC, which were mainly influenced by human activities. $\delta^{15}\text{N}_{\text{TN}}$ distribution shows that TN in the east side of PRE mainly originated from industrial wastewater input from the Pearl River, while in the east side TN was mainly from domestic sewage discharge. Additionally, since the 1990s, the source of BC has shifted from biomass combustion to predominantly fossil fuel emissions. Isotopic quantification by the IsoSource model reveals that nearly 70% of BC originates from fossil fuels and C3 plant combustion; this underscores the significant impact of human activities on the distribution of organic carbon in the PRE and its adjacent areas.

Data availability statement

The original contributions presented in the study are included in the article/supplementary material. Further inquiries can be directed to the corresponding author/s.

Author contributions

RC: Data curation, Methodology, Visualization, Writing – original draft, Writing – review & editing. QL: Data curation, Formal analysis, Writing – original draft, Writing – review & editing. CH: Writing – review & editing. JH: Data curation, Investigation, Writing – review & editing. GJ: Visualization, Writing – review & editing. XL: Writing – review & editing. MC: Writing – review & editing. CC: Methodology, Writing – review & editing. FC: Conceptualization, Funding acquisition, Project administration, Validation, Writing – review & editing.

Funding

The author(s) declare that financial support was received for the research, authorship, and/or publication of this article. This study was supported by the Basic and Applied Basic Research Foundation of Guangdong Province (2023B1515120029), National Natural Science Foundation of China (42073074, 92158201), and Innovation and Entrepreneurship Project of Shantou (2021112176541391).

Acknowledgments

We would like to thank professor Gangjian Wei and Feng Ye for their support in collecting water samples.

References

- Atwood, T. B., Witt, A., Mayorga, J., Hammill, E., and Sala, E. (2020). Global patterns in marine sediment carbon stocks. *Front. Mar. Sci.* 7, 165. doi: 10.3389/fmars.2020.00165
- Biggs, R. B., and Howell, B. A. (1984). "The estuary as a sediment trap: alternate approaches to estimating its filtering efficiency," in *Estuary as a Filter*, Academic Press 107–129. doi: 10.1016/B978-0-12-405070-9.50012-8
- Bucheli, T. D., Blum, F., Desaulles, A., and Gustafsson, Ö. (2004). Polycyclic aromatic hydrocarbons, black carbon, and molecular markers in soils of Switzerland. *Chemosphere* 56, 1061–1076. doi: 10.1016/j.chemosphere.2004.06.002
- Carneiro, L. M., do Rosário Zucchi, M., de Jesus, T. B., da Silva Júnior, J. B., and Hadlich, G. M. (2021). [$\delta^{13}C$, $\delta^{15}N$ and TOC/TN as indicators of the origin of organic matter in sediment samples from the estuary of a tropical river. *Mar. pollut. Bull.* 172, 112857. doi: 10.1016/j.marpolbul.2021.112857
- Chen, F., Deng, Z., Lao, Q., Bian, P., Jin, G., Zhu, Q., et al. (2022). Nitrogen cycling across a salinity gradient from the pearl river estuary to offshore: insight from nitrate dual isotopes. *J. Geophysical Research: Biogeosciences* 127, e2022JG006862. doi: 10.1029/2022jg006862
- Coppola, A. I., Wagner, S., Lennartz, S. T., Seidel, M., Ward, N. D., Dittmar, T., et al. (2022). The black carbon cycle and its role in the Earth system. *Nat. Rev. Earth Environ.* 3, 516–532. doi: 10.1038/s43017-022-00316-6
- Dai, M., Su, J., Zhao, Y., Hofmann, E. E., Cao, Z., Cai, W. J., et al. (2022). Carbon fluxes in the coastal ocean: synthesis, boundary processes, and future trends. *Annu. Rev. Earth Planetary Sci.* 50, 593–626. doi: 10.1146/annurev-earth-032320-090746
- Dan, S. F., Cui, D., Yang, B., Wang, X., Ning, Z., Lu, D., et al. (2022). Sources, burial flux and mass inventory of black carbon in surface sediments of the Daya Bay, a typical mariculture bay of China. *Mar. pollut. Bull.* 179, 113708. doi: 10.1016/j.marpolbul.2022.113708
- Deng, Y., Liu, Z., Zu, T., Hu, J., Gan, J., Lin, Y., et al. (2022). Climatic controls on the interannual variability of shelf circulation in the northern South China Sea. *J. Geophysical Research: Oceans* 127, e2022JC018419. doi: 10.1029/2022jc018419
- Dickens, A. F., Gélinais, Y., and Hedges, J. I. (2004). Physical separation of combustion and rock sources of graphitic black carbon in sediments. *Mar. Chem.* 92, 215–223. doi: 10.1016/j.marchem.2004.06.027
- Faust, J. C., Tessin, A., Fisher, B. J., Zindorf, M., Papadaki, S., Hendry, K. R., et al. (2021). Millennial scale persistence of organic carbon bound to iron in Arctic marine sediments. *Nat. Commun.* 12, 275. doi: 10.1038/s41467-020-20550-0
- Folk, R. L., and Ward, W. C. (1957). Brazos River bar [Texas]; a study in the significance of grain size parameters. *J. Sedimentary Res.* 27 (1), 3–26. doi: 10.1306/74d70646-2b21-11d7-8648000102c1865d
- Fontugne, M. R., and Jouanneau, J. M. (1987). Modulation of the particulate organic carbon flux to the ocean by a macrotidal estuary: evidence from measurements of carbon isotopes in organic matter from the Gironde system. *Estuarine Coast. Shelf Sci.* 24, 377–387. doi: 10.1016/0272-7714(87)90057-6
- Fu, W., Qi, Y., Luo, C., Zhang, H., and Wang, X. (2023). Distinct radiocarbon ages reveal two black carbon pools preserved in large river estuarine sediments. *Environ. Sci. Technol.* 57, 6216–6227. doi: 10.1021/acs.est.2c09079
- Gao, L., Yao, P., Wang, J., and Zhao, B. (2016). Distribution and sources of organic carbon in surface sediments from the Bohai Sea. *Haiyang Xuebao* 38, 8–20. doi: 10.3969/j.issn.0253-4193.2016.06.002
- Gu, Y., Wang, C., Lü, S., Yang, Y., Feng, J., Fang, J., et al. (2010). Distribution and pollution assessment of biogenic sediments in surface sediments in Western Guangdong. *J. Shenzhen Univ. (science technology)* 27, 347–353.
- Huang, C., Chen, F., Zhang, S., Chen, C., Meng, Y., Zhu, Q., et al. (2020). Carbon and nitrogen isotopic composition of particulate organic matter in the Pearl River Estuary and the adjacent shelf. *Estuarine Coast. Shelf Sci.* 246, 107003. doi: 10.1016/j.eccs.2020.107003
- Huang, C., Lao, Q., Chen, F., Zhang, S., Chen, C., Bian, P., et al. (2021). Distribution and sources of particulate organic matter in the Northern South China Sea: Implications of human activity. *J. Ocean Univ. China* 20, 1136–1146. doi: 10.1007/s11802-021-4807-z
- Lao, Q., Chen, F., Jin, G., Lu, X., Chen, C., Zhou, X., et al. (2023a). Characteristics and mechanisms of typhoon-induced decomposition of organic matter and its implication for climate change. *J. Geophysical Research: Biogeosciences* 128, e2023JG007518. doi: 10.1029/2023jg007518
- Lao, Q., Zhang, S., Li, Z., Chen, F., Zhou, X., Jin, G., et al. (2022). Quantification of the seasonal intrusion of water masses and their impact on nutrients in the Beibu Gulf using dual water isotopes. *J. Geophysical Research: Oceans* 127, e2021JC018065. doi: 10.1029/2021JC018065
- Lao, Q., Chen, F., Liu, G., Chen, C., Jin, G., Zhu, Q., et al. (2019). Isotopic evidence for the shift of nitrate sources and active biological transformation on the western coast of Guangdong Province, South China. *Mar. pollut. Bull.* 142, 603–612. doi: 10.1016/j.marpolbul.2019.04.026
- Lao, Q., Liu, S., Ling, Z., Jin, G., Chen, F., Chen, C., et al. (2023b). External dynamic mechanisms controlling the periodic offshore blooms in Beibu Gulf. *J. Geophysical Research: Oceans* 128, e2023JC019689. doi: 10.1029/2023jc019689
- Lao, Q., Lu, X., He, G., Li, H., Chen, F., Jin, G., et al. (2024). Winter monsoon brings substantial terrestrial aerosols to Bay of Bengal and adjacent Indian Ocean: Insights from carbon and nitrogen isotopes. *Atmospheric Environ.* 329, 120555. doi: 10.1016/j.atmosenv.2024.120555
- LaRowe, D. E., Arndt, S., Bradley, J. A., Estes, E. R., Hoarfrost, A., Lang, S. Q., et al. (2020). The fate of organic carbon in marine sediments—New insights from recent data and analysis. *Earth-Science Rev.* 204, 103146. doi: 10.1016/j.earscirev.2020.103146
- Li, R., Liang, Z., Hou, L., Zhang, D., Wu, Q., Chen, J., et al. (2023). Revealing the impacts of human activity on the aquatic environment of the Pearl River Estuary, South China, based on sedimentary nutrient records. *J. Cleaner Production* 385, 135749. doi: 10.1016/j.jclepro.2022.135749
- Li, Y., Song, G., Massicotte, P., Yang, F., Li, R., and Xie, H. (2019). Distribution, seasonality, and fluxes of dissolved organic matter in the Pearl River (Zhujiang) estuary, China. *Biogeosciences* 16, 2751–2770. doi: 10.5194/bg-16-2751-2019
- Lim, B., and Cachier, H. (1996). Determination of black carbon by chemical oxidation and thermal treatment in recent marine and lake sediments and Cretaceous-Tertiary clays. *Chem. Geology* 131, 143–154. doi: 10.1016/0009-2541(96)00031-9
- Liu, L., Li, Q., Huang, M., and Yang, Y. (2019). Carbon concentration and isotope composition of black carbon in the topsoil of the central and southeastern Qinghai-Tibetan Plateau, and their environmental significance. *Catena* 172, 132–139. doi: 10.1016/j.catena.2018.08.011
- Liu, X., Li, Y., Lin, T., Guo, N., Yuan, J., Yang, Y., et al. (2024). Characterizing sedimentary black carbon in the Pearl River Estuary, Southern China. *Mar. Chem.* 261, 104383. doi: 10.1016/j.marchem.2024.104383

Conflict of interest

The authors declare that the research was conducted in the absence of any commercial or financial relationships that could be construed as a potential conflict of interest.

Publisher's note

All claims expressed in this article are solely those of the authors and do not necessarily represent those of their affiliated organizations, or those of the publisher, the editors and the reviewers. Any product that may be evaluated in this article, or claim that may be made by its manufacturer, is not guaranteed or endorsed by the publisher.

- Marlon, J. R., Bartlein, P. J., Carcaillet, C., Gavin, D. G., Harrison, S. P., Higuera, P. E., et al. (2008). Climate and human influences on global biomass burning over the past two millennia. *Nat. Geosci.* 1, 697–702. doi: 10.1038/ngeo313
- Meyers, P. A. (1994). Preservation of elemental and isotopic source identification of sedimentary organic matter. *Chem. geology* 114, 289–302. doi: 10.1016/0009-2541(94)90059-0
- O'Leary, M. H. (1988). Carbon isotopes in photosynthesis. *Bioscience* 38, 328–336. doi: 10.2307/1310735
- Pang, Y., Zhou, B., Zhou, X., Xu, X., Liu, X., Zhan, T., et al. (2021). Abundance and $\delta^{13}\text{C}$ of sedimentary black carbon indicate rising wildfire and C4 plants in Northeast China during the early Holocene. *Palaeogeography Palaeoclimatology Palaeoecol.* 562, 110075. doi: 10.1016/j.palaeo.2020.110075
- Ruellan, S., and Cachier, H. (2001). Characterisation of fresh particulate vehicular exhausts near a Paris high flow road. *Atmospheric Environ.* 35, 453–468. doi: 10.1016/S1352-2310(00)00110-2
- Song, W., Liu, X. Y., Hu, C. C., Chen, G. Y., Liu, X. J., Walters, W. W., et al. (2021). Important contributions of non-fossil fuel nitrogen oxides emissions. *Nat. Commun.* 12, 243. doi: 10.1038/s41467-020-20356-0
- Sun, X., Hu, L., Hu, B., Sun, X., Wu, X., Bi, N., et al. (2022). Remarkable signals of the ancient Chinese civilization since the Early Bronze Age in the marine environment. *Sci. Total Environ.* 804, 150209. doi: 10.1016/j.scitotenv.2021.150209
- Sun, X., Song, J., Zhang, G., and Hu, J. (2008). Sedimentary record of black carbon in the Pearl River estuary and adjacent northern South China Sea. *Appl. Geochemistry* 23, 3464–3472. doi: 10.1016/j.apgeochem.2008.08.006
- Uchida, M., Mantoku, K., Kumata, H., Kaneyasu, N., Handa, D., Arakaki, T., et al. (2023). Source apportionment of black carbon aerosols by isotopes (^{14}C and ^{13}C) and Bayesian modeling from two remote islands in east Asian outflow region. *Nucl. Instruments Methods Phys. Res. Section B: Beam Interact. Materials Atoms* 538, 64–74. doi: 10.1016/j.nimb.2023.02.002
- Vaezzadeh, V., Zhong, G., Gligorovski, S., Wang, Y., and Zhang, G. (2023). Characteristics of dissolved black carbon in riverine surface microlayer. *Mar. pollut. Bull.* 194, 115301. doi: 10.1016/j.marpolbul.2023.115301
- Wei, B., Mollenhauer, G., Hefter, J., Grotheer, H., and Jia, G. (2020). Dispersal and aging of terrigenous organic matter in the Pearl River Estuary and the northern South China Sea Shelf. *Geochimica Cosmochimica Acta* 282, 324–339. doi: 10.1016/j.gca.2020.04.032
- Wu, J., Chen, J., Wang, C., Yan, X., Yin, X., and Liu, Q. (2023). Constraining the origin of sedimentary organic matter in the eastern Guangdong coast of China using $\delta^{13}\text{C}$ and $\delta^{15}\text{N}$. *Front. Mar. Sci.* 10, 1234116. doi: 10.3389/fmars.2023.1234116
- Wu, Y., Ya, M., Chen, H., Li, Y., Guo, W., and Wang, X. (2019). Distribution and isotopic composition of sedimentary black carbon in a subtropical estuarine-coastal region of the western Taiwan Strait: Implications for tracing anthropogenic inputs. *Sci. Total Environ.* 684, 509–518. doi: 10.1016/j.scitotenv.2019.05.165
- Xia, J., Han, Y., Tan, J., Abarike, G. A., and Song, Z. (2022). The characteristics of organic carbon in the offshore sediments surrounding the Leizhou Peninsula, China. *Front. Earth Sci.* 10, 648337. doi: 10.3389/feart.2022.648337
- Xia, S., Song, Z., Li, Q., Guo, L., Yu, C., Singh, B. P., et al. (2021). Distribution, sources, and decomposition of soil organic matter along a salinity gradient in estuarine wetlands characterized by C: N ratio, $\delta^{13}\text{C}$ - $\delta^{15}\text{N}$, and lignin biomarker. *Global Change Biol.* 27, 417–434. doi: 10.1111/gcb.15403
- Xiao, H. W., Mao, D. Y., Huang, L. L., Xiao, H. Y., and Wu, J. F. (2021). Evaluation of black carbon source apportionment based on one year's daily observations in Beijing. *Sci. Total Environ.* 773, 145668. doi: 10.1016/j.scitotenv.2021.145668
- Xiao, H., Shahab, A., Ye, F., Wei, G., Li, J., and Deng, L. (2022). Source-specific ecological risk assessment and quantitative source apportionment of heavy metals in surface sediments of Pearl River Estuary, China. *Mar. pollut. Bull.* 179, 113726. doi: 10.1016/j.marpolbul.2022.113726
- Yang, Y., Li, Y., Huang, C., Chen, F., Chen, C., Zhang, H., et al. (2023). Anthropogenic influences on the sources and distribution of organic carbon, black carbon, and heavy metals in Daya Bay's surface sediments. *Mar. pollut. Bull.* 196, 115571. doi: 10.1016/j.marpolbul.2023.115571
- Ye, F., Guo, W., Shi, Z., Jia, G., and Wei, G. (2017). Seasonal dynamics of particulate organic matter and its response to flooding in the Pearl River Estuary, China, revealed by stable isotope ($\delta^{13}\text{C}$ and $\delta^{15}\text{N}$) analyses. *J. Geophysical Research: Oceans* 122, 6835–6856. doi: 10.1002/2017JC012931
- Ye, F., Guo, W., Wei, G., and Jia, G. (2018). The sources and transformations of dissolved organic matter in the Pearl River Estuary, China, as revealed by stable isotopes. *J. Geophysical Research: Oceans* 123, 6893–6908. doi: 10.1029/2018JC014004
- Ye, F., Jia, G., Xie, L., Wei, G., and Xu, J. (2016). Isotope constraints on seasonal dynamics of dissolved and particulate N in the Pearl River Estuary, south China. *J. Geophysical Research: Oceans* 121, 8689–8705. doi: 10.1002/2016JC012066
- Ye, F., Ni, Z., Xie, L., Wei, G., and Jia, G. (2015). Isotopic evidence for the turnover of biological reactive nitrogen in the Pearl River Estuary, south China. *J. Geophysical Research: Biogeosciences* 120, 661–672. doi: 10.1002/2014jg002842
- Ye, X., Chen, J., Wang, A., Huang, C., Wang, W., and Li, D. (2011). Sources and burial of carbon in sediments from the Western Taiwan Strait. *Acta Oceanologica Sin.* 33, 73–82.
- Yin, X., Lin, Y., Li, Y., Wang, L., Sun, Z., and Li, G. (2021). Sulfate reduction and its important role in organic carbon mineralization in sediments of the Pearl River Estuary. *Estuarine Coast. Shelf Sci.* 260, 107511. doi: 10.1016/j.ecss.2021.107511
- Yu, F., Zong, Y., Lloyd, J. M., Huang, G., Leng, M. J., Kendrick, C., et al. (2010). Bulk organic $\delta^{13}\text{C}$ and C/N as indicators for sediment sources in the Pearl River delta and estuary, southern China. *Estuarine Coast. Shelf Sci.* 87, 618–630. doi: 10.1016/j.ecss.2010.02.018
- Zhang, L., Yin, K., Wang, L., Chen, F., Zhang, D., and Yang, Y. (2009). The sources and accumulation rate of sedimentary organic matter in the Pearl River Estuary and adjacent coastal area, Southern China. *Estuarine Coast. Shelf Sci.* 85, 190–196. doi: 10.1016/j.ecss.2009.07.035
- Zhang, Q., Zhou, J., Fang, Z., Yang, W., Chen, M., and Zheng, M. (2024). Sources and dynamics of dissolved black carbon in the Pearl River Estuary and Shelf, Northern South China Sea. *J. Oceanography* 80, 71–83. doi: 10.1007/s10872-023-00708-2
- Zhang, T., Li, X., Lan, H., Sun, S., and Jiang, Z. (2014). Distribution characteristics and influencing factors of lignin in surface sediments of the yellow sea. *Mar. Environ. Sci.* 33, 822–829.
- Zhao, B., Yao, P., Bianchi, T. S., and Yu, Z. G. (2021). Controls on organic carbon burial in the Eastern China marginal seas: A regional synthesis. *Global Biogeochemical Cycles* 35, e2020GB006608. doi: 10.1029/2020gb006608
- Zhou, X., Zhang, S., Liu, S., Chen, C., Lao, Q., and Chen, F. (2024). Thermal fronts in coastal waters regulate phytoplankton blooms via acting as barriers: A case study from western Guangdong, China. *J. Hydrology* 636, 131350. doi: 10.1016/j.jhydrol.2024.131350